

UDC 541.6:548.737

**ADSORPTION BEHAVIOR OF CO AND C₂H₂ ON THE GRAPHITE BASAL SURFACE:
A QUANTUM CHEMISTRY STUDY****T. Hosseinnejad¹, R. Abdullah Mirzaei², F. Nazari², M.H. Karimi-Jafari³**¹*Department of Chemistry, Faculty of Science, Alzahra University, Vanak, Tehran, Iran*

E-mail: tayeb.hosseinnejad@alzahra.ac.ir

²*Department of Chemistry, Faculty of Science, Shahid Rajaee Teacher Training University, Tehran, Iran*³*Institute of Biochemistry and Biophysics, University of Tehran, Iran*

Received April, 9, 2012

Revised — July, 29, 2012

The adsorption of CO and C₂H₂ molecules on the perfect basal surface of graphite is investigated by adopting cluster models in conjunction with quantum chemical calculations. The non-covalent interaction potential energy curves for three different orientations of CO and C₂H₂ molecules with respect to the inert basal plane of graphite are calculated via semi-empirical and Möller-Plesset *ab initio* methods. Then, we have considered the effects of interaction energies on the C≡O and C≡C bond lengths by performing the partial geometry optimization procedure on the CO-graphite and C₂H₂-graphite systems in various intermolecular distances. The computational analysis of all physical noncovalent potential energy curves reveals that the relative configurations in which CO and C₂H₂ molecules approach the graphite sheet from out of the plane have stronger interaction energy and so is more favorable from the energetic viewpoint. This means that the graphite layer prefers to increase its thickness via the chemical vapor deposition of CO and C₂H₂ on the graphite.

Keywords: graphite basal surface, carbon monoxide, acetylene, physical interaction energy, quantum chemical calculations.

INTRODUCTION

The recent advances in experimental techniques and the ever-growing interest in nanotechnology applications brought considerable attention to graphite systems. One of the most important methods of producing carbon materials is chemical vapor deposition (CVD) on graphite surface. In the recent years much attention to the growth of carbon materials, such as carbon fibers, carbon nanotubes [1, 2], pyrolytic carbons [3, 4], and carbon nanospheres (that are all related mainly to graphite structures) by performing the catalytic CVD procedure. In this technique, carbon monoxide and acetylene are widely used as appropriate substrates.

It should be stated that the extended honeycomb structure model of graphite surface is the basic building block of other important allotropes such as 3D graphite, 1D nanotubes, and 0D fullerene. So, we have chosen polycyclic aromatic hydrocarbons to model the adsorption of CO and C₂H₂ molecules on graphite nanolayers. These polycyclic aromatic hydrocarbons themselves are of great research interest due to their high stability, rigid planar structure, and characteristic optical spectra [5, 6].

In general, the adsorption on planar surfaces is classified into two categories. One is the physisorption on a perfect surface that is chemically inert towards the adsorption and dissociation of small molecules, and another is chemisorption that happens on defective reactive surfaces and thus contributes to catalytic reactions. It is well known from previous experimental observations that small mo-

lecular species only physisorb on the clean graphite basal surface with the corresponding low binding energy [7, 8].

From the theoretical viewpoint, in some previous systematic investigations [28, 29] Xu and co-workers have studied computationally the adsorption interactions and dissociative adsorption reaction of water, CO_x, and NO_x (x = 1, 2) on the (0001) graphite surface using the ONIOM integrated method [30]. Firstly, they have selected the B3LYP/6-31+G* hybrid density functional method as high level theory for the C₂₄H₁₂ + CO_x/NO_x model system and then a less expensive self-consistent charge density functional tight binding plus London dispersion (DFTB-D) method [31, 32] was employed to include the horizontal π -conjugation effects. They have also chosen a C₉₄H₂₄ dicircumcoronene graphene slab as a model system for the graphite surface in a finite-size molecular structure. They have predicted the potential energy surface (PES) for the dissociative adsorption reaction of CO_x/NO_x with the graphite slab surface and calculated their corresponding reaction rate constants at high temperatures and pressures using the PES data in RRKM computations [33].

In another theoretical study, Zhang and coworkers [34] have investigated the interactions between perfect, doped, and defective graphenes with small gas molecules (CO, NO, NO₂, and NH₃) using density functional computations [35] with the plane-wave basis set and the periodic boundary condition. In the case of CO on the graphene surface, the adsorption energy and the distance between CO and a graphene sheet in basal and doped models have been calculated to be around -0.15 eV and 3 Å respectively. On the other hand, the adsorption energy and the distance between CO and a defective graphene sheet have been obtained of about -2.3 eV and 1.3 Å respectively. So, they have indicated that defective graphene is more suitable for sensing CO than basal and doped graphene.

In this research, we have mainly focused on the theoretical effective cluster model of a basal graphite layer and its growth via the pyrolysis reaction of CO and C₂H₂ from the structural and energetic viewpoints. In this respect, we calculated the physical interaction potential energies at several orientations of CO and C₂H₂ molecules with respect to the basal graphite surface via the semi-empirical and Möller-Plesset *ab initio* quantum chemistry methods [9]. It is important to note that these relative configurations may have different contributions to the primary interactions between molecular species and graphite and consequently to the determination of the precursor structure of the reaction complex in the chemical vapor deposition process. Additionally, we analyzed the ability of three various semi-empirical quantum mechanical techniques for the accurate description of physical interactions in noncovalent molecular systems such as CO-graphite and C₂H₂-graphite.

It should be stated that the choice of the Möller-Plesset *ab initio* method for the prediction of noncovalent physical interactions was motivated by the facts that the London dispersion energy plays a key role in this type of interactions and consequently it requires the use of the procedure by including a large portion of the electronic correlation energy together with an extended atomic orbital (AO) basis set.

Furthermore, we have investigated the effect of potential interaction energies on the C≡O and C≡C bond lengths while CO and C₂H₂ molecules are approaching the graphite sheet with different relative orientations. A comparative study on the obtained physical interaction potential energy curves of CO-graphite and C₂H₂-graphite systems demonstrates that the orientations in which CO and C₂H₂ molecules approach the graphite sheet from out of the plane have the stronger interaction potential energy and consequently suggests that graphite prefers to grow from its surface and so increases its thickness in CVD of carbon monoxide and acetylene.

COMPUTATIONAL DETAILS

As the first step in the survey of physical interaction potential energies between CO and C₂H₂ molecules with a graphite layer, we have employed a planar polyaromatic molecule as an inert basal graphite model. By choosing this model, the graphite system is reduced to a computational tractable size. It was discussed in [10, 11] that this size of the graphite model provides a reliable and accurate representation for the structural and energetic features of the graphite surface. It is noteworthy that in a previous computational study [7], the reliability of the graphite model adopted in our present study

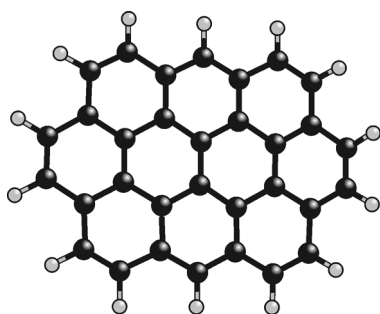


Fig. 1. Schematic representation of the basal structure for the graphite sheet

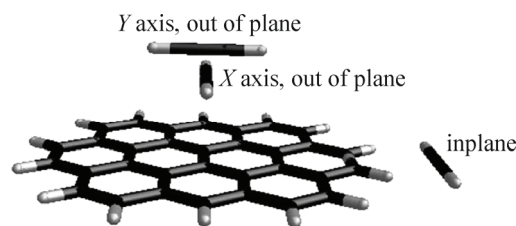


Fig. 2. Three different relative orientations of molecular species with respect to the basal graphite plane

has been verified by a comparative study of larger planar polyaromatic models. A schematic structure of this basal model has been shown in Fig. 1. The boundaries of this model were saturated with hydrogen atoms, which is a typical procedure for covalent materials [12].

In the next step, three different relative orientations were considered for the approach of CO and C₂H₂ molecules towards the graphite basal surface: two of them are out of the plane and the other is in the plane of the graphite sheet. These orientations have been chosen based on the active sites of the graphite surface and are illustrated in Fig. 2.

All calculations were carried out in the framework of AM1 [13], PM3 [14, 15], and PM6 [16] semi-empirical methods and the second-order Möller-Plesset (MP2) *ab initio* level of theory [17] together with the 6-31++G** basis set [18—21] for all atoms. It should be emphasized that AM1 and PM3 semi-empirical methods are not accurate enough for the energetic description of noncovalent interactions for many reasons: i) parametrization for only a limited number of atoms and ii) overestimated stabilization energies for optimized geometries especially in H-bonded complexes. On the other hand, the new PM6 method is superior to other semi-empirical quantum mechanical methods in various aspects. It is an NDDO-based method improved by the adoption of Voityuk's core-core diatomic interaction term [22] and Thiel's *d*-orbital approximation [23, 24]. These modifications allowed the parametrization of 80 elements and also reduced the error for main group elements. So, one of the most important goals of this research is to examine the ability of the PM6 method in the prediction of physical interaction energies in comparison with AM1 and PM3 semi-empirical methods and the MP2 *ab initio* approach.

All MP2 interaction potential energies were corrected for the basis set superposition error via the standard counterpoise procedure [25]. In semi-empirical calculations, the convergence criteria for the SCF procedure was adopted as 10⁻¹⁰ kcal·mol⁻¹. All MP2 computations were performed using the GAMESS suite of programs [26] and the MOPAC 2009 software [27] was utilized for the semi-empirical calculations.

RESULTS AND DISCUSSION

The interaction energy at each distance *R*, were defined according to the expression

$$\Delta E_{\text{int}}(R) = E(\text{G-m}) - E(\text{G}) - E(\text{m}),$$

where *E*(*m*) is the energy of an isolated molecule, *E*(*G*) is the energy at its optimized relaxed geometry in the absence of adsorbed species, and *E*(*G-m*) corresponds to the energy of CO-graphite and C₂H₂-graphite complexes at a distance *R*, and a negative ΔE_{int} value means a stable structure in energy.

Firstly, the adsorption of CO and C₂H₂ molecules on the graphite surface has been considered in three relative configurations for the basal structure model of graphite. The CO-graphite and C₂H₂-graphite interaction potential energy curves derived from AM1, PM3, and PM6 computations for three different orientations (displayed in Fig. 2) are plotted in Fig. 3, *a—c* and Fig. 4, *a—c* respectively. A qualitative analysis of the aforementioned figures depicts that some of the potential curves obtained with AM1 and PM3 methods are not well-behaved functions of *R* so that some of potential curves

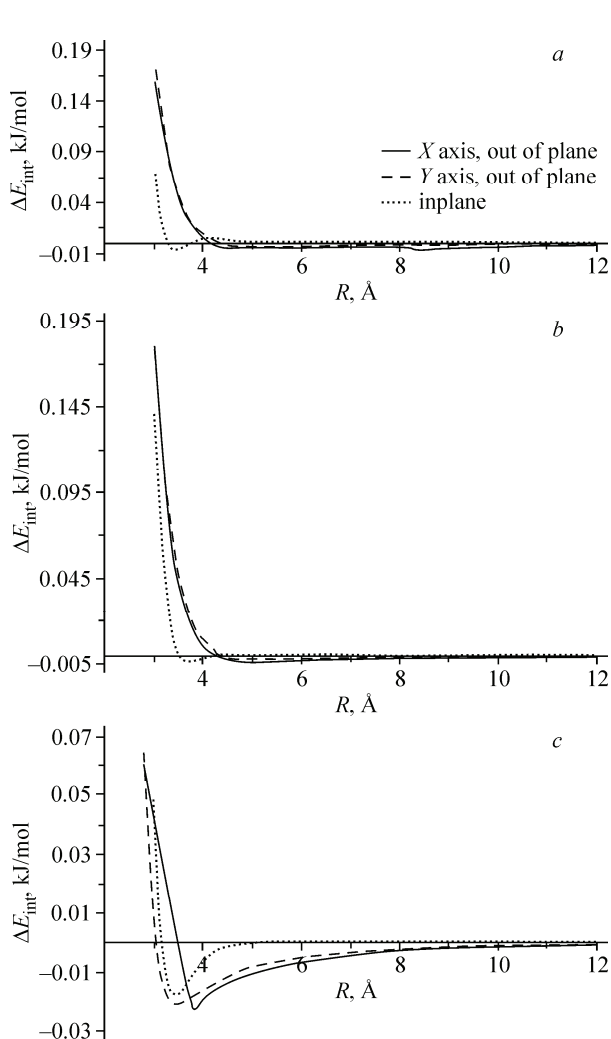


Fig. 3. Physical interaction potential energy curves for three different relative orientations of CO molecule calculated using AM1 (a), PM3 (b), and PM6 (c) semi-empirical methods

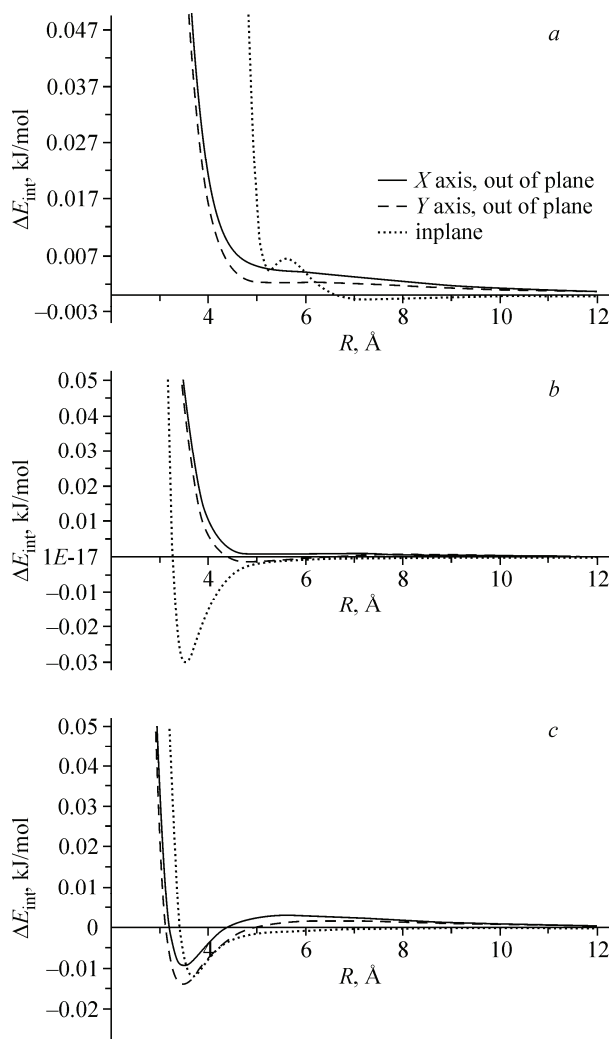


Fig. 4. Physical interaction potential energy curves for three different relative orientations of the C_2H_2 molecule calculated using AM1 (a), PM3 (b), and PM6 (c) semi-empirical methods

show a barrier before or after reaching the potential minimum point. Meanwhile, all of the potential energy curves for three different orientations obtained with PM6 calculations have a typical and well-behaved potential well.

As already discussed, these findings confirmed the relative success of the PM6 method compared to AM1 and PM3 techniques in the description of noncovalent physical interactions between CO and C_2H_2 molecules with the graphite surface. Thus, the rest of this article is devoted to the results obtained with PM6 computations.

It is important to state that the order of contributions to the overall physical interaction for different orientations can be determined based on their minimum point (equilibrium) energies. Strictly speaking, the relative orientations with the deeper potential well should possess the larger contribution in the pyrolytic reaction of CVD process.

As it can be seen from Figs. 3, c and 4, c, among the aforementioned three structures, the orientations in which CO and C_2H_2 molecules approach the graphite sheet from out of the plane have a stronger interaction potential compared to the other orientation. However, the calculated values of potential energies for the interaction of CO and C_2H_2 with the basal surface of graphite reveal that CO and C_2H_2 species can only be physisorbed on the perfect basal graphite sheet while the potential ener-

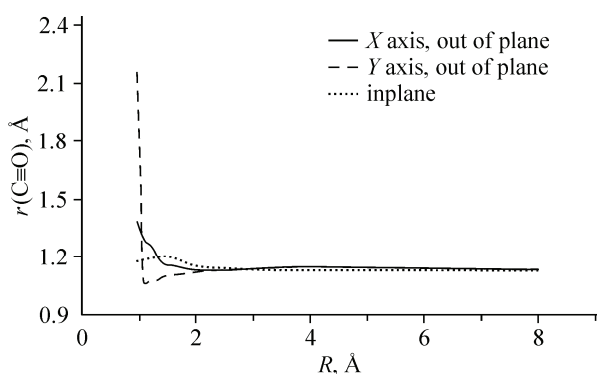


Fig. 5. Variation of the C≡O bond length as a function of the intermolecular distance for three different relative orientations of the CO molecule with respect to the basal graphite surface

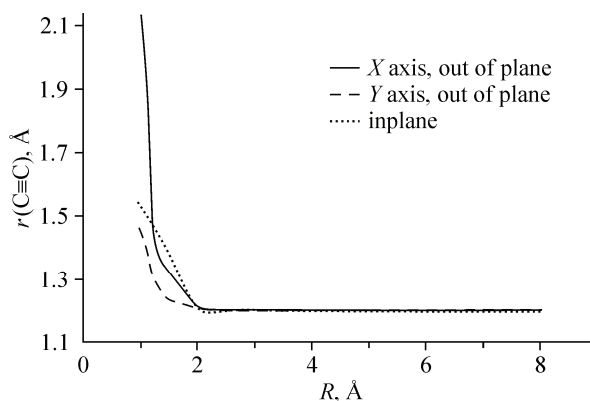
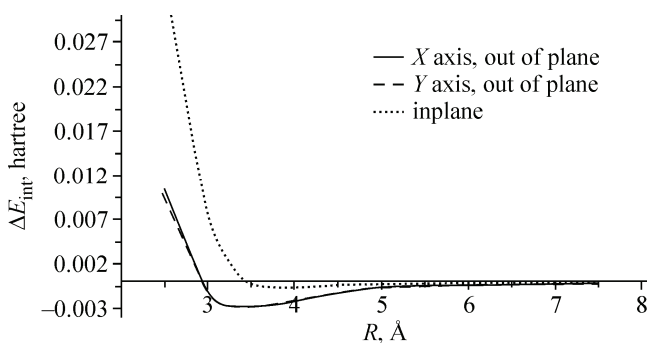


Fig. 6. Variation of the C≡C bond length as a function of the intermolecular distance for three different relative orientations of the C₂H₂ molecule with respect to the basal graphite surface

gy well depth is about 0.02 kJ/mol at the PM6 level, suggesting a weak nature of noncovalent interactions.

In the next step, we have investigated the effect of potential interaction energies on the C≡O and C≡C bond distances while CO and C₂H₂ molecules are closing to the graphite basal sheet. It should be noticed that during this process, we have only relaxed the C≡O and C≡C bond lengths while all the other structural parameters have been frozen. The variations of calculated C≡O and C≡C bond lengths have been illustrated in Figs. 5 and 6 respectively as a function of intermolecular distances. Figs. 5 and 6 depict clearly that for intermolecular distances larger than 2 Å the C≡O and C≡C bond lengths do not change considerably while their values are about 1.13 Å and 1.20 Å respectively, the same as those of calculated free CO and C₂H₂ in the gas phase. This behavior can be essentially due to the weak nature of physical interactions between CO and C₂H₂ molecules with the basal surface of graphite. Moreover, for the shorter intermolecular distances, the C≡O and C≡C bond lengths were elongated to ~2 Å, which indicated that the adsorbed CO and C₂H₂ species are chemically activated and the chemical adsorption can occur at close intervals to the basal graphite surface.

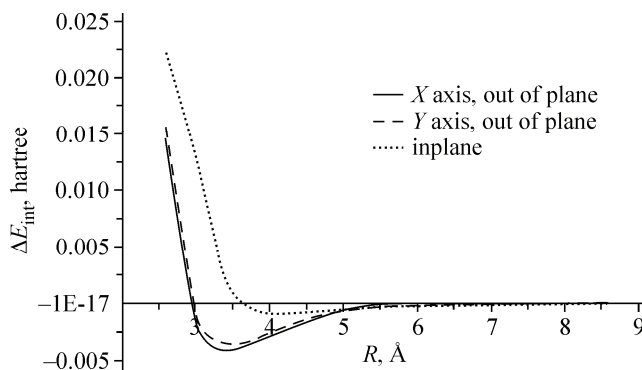
In order to achieve a more reliable description for noncovalent physical interactions between CO and C₂H₂ molecules with the basal graphite surface we have calculated the interaction energy values via the MP2 *ab initio* method for three different relative configurations. In Figs. 7 and 8, the CO-graphite and C₂H₂-graphite interaction potential energy curves derived from the MP2 computations have been illustrated respectively. In Table 1, we have reported the equilibrium distance R_e at the minimum point of the potential energy curves and its corresponding interaction energy ΔE_e obtained from the MP2 calculation for three different relative orientations in CO-graphite and C₂H₂-graphite systems. The reported Table 1 results clearly show that i) the orientations in which CO and C₂H₂ molecules approach the graphite sheet from out of the plane have a considerably deeper potential well in comparison with the other orientation and ii) there is a little distinction in the behavior of potential energy



curves between two relative orientations in which CO and C₂H₂ molecules approach the graphite sheet from out of the plane (as represented in Figs. 7 and 8). We have also assessed and compared the ability of PM6 and

Fig. 7. MP2/6-31++G** calculated physical interaction potential energy curves for three different orientations of the CO molecule with respect to the basal graphite surface

Fig. 8. MP2/6-31++G** calculated physical interaction potential energy curves for three different orientations of the C_2H_2 molecule with respect to the basal graphite surface



MP2 methods for a reliable quantitative description of noncovalent interactions. In Table 2, we have presented R_e and ΔE_e values calculated at the PM6 and MP2/6-31++G** levels of theory for three relative orientations in CO-graphite and C_2H_2 -graphite systems. It

can be clearly derived from the reported Table 2 results that the PM6 approach is inadequate for an accurate quantitative representation of interactions in comparison with the MP2 method. Indeed, the PM6 interaction energies are about 0.01–0.02 kJ/mol while MP2 calculated ones are about 7–11 kJ/mol.

In overall, based on MP2 and semi-empirical results, the orientation in which CO and C_2H_2 molecules approach the basal graphite sheet in the plane not only has a weaker interaction energy, but also this orientation has a considerably shallower potential well in comparison with the other orientations, which can be seen more clearly in the MP2 computations.

CONCLUSIONS

To summarize, semi-empirical and MP2 *ab initio* molecular orbital calculations have been performed to study and analyze the adsorption behavior of CO and C_2H_2 molecules on the basal cluster model of graphite from the energetic and structural viewpoints. A comparative study on the calculated

Table 1

Equilibrium distance R_e at the minimum point of the potential energy curves and its corresponding interaction energy ΔE_e obtained from MP2 calculations for three different relative orientations in CO-graphite and C_2H_2 -graphite systems

Orientation	CO-graphite		C_2H_2 -graphite	
	R_e , Å	ΔE_e , hartree	R_e , Å	ΔE_e , hartree
X axis, out of plane	3.5	-0.00279	3.4	-0.00418
Y axis, out of plane	3.5	-0.00281	3.6	-0.00359
In plane	4	-0.00068	4	-0.00085

Table 2

*PM6 and MP2/6-31++G** calculated values of R_e and ΔE_e for three different relative orientations of CO-graphite (CO—G) and C_2H_2 -graphite (C_2H_2 —G) systems.*

The definitions of R_e and ΔE_e are the same as in Table 1

Computational method	X axis, out of plane		Y axis, out of plane		In plane	
	CO—G	C_2H_2 —G	CO—G	C_2H_2 —G	CO—G	C_2H_2 —G
PM6						
R_e , Å	3.8	3.5	3.5	3.5	3.5	3.8
ΔE_e , kJ/mol	-0.0234	-0.00925	-0.0209	-0.0144	-0.0178	-0.0125
MP2/6-31++G**						
R_e , Å	3.5	3.4	3.5	3.6	4	4
ΔE_e , kJ/mol	-7.3251	-10.9745	-7.3776	-9.4255	-1.7853	-2.2316

noncovalent interaction potential energy curves of CO-graphite and C₂H₂-graphite systems shows that i) the PM6 method can provide a qualitatively more reliable theoretical description of noncovalent interactions in comparison with AM1 and PM3 techniques, but it is not superior to the MP2 *ab initio* method for providing an accurate quantitative description and ii) the relative configurations in which CO and C₂H₂ molecules approach the basal graphite sheet from out of the plane have a more potential well depth and consequently depict stronger interactions. Therefore, based on the obtained PM6 and MP2 results, we predict that graphite prefers to grow from its surface and so increases its thickness in CVD of carbon monoxide and acetylene.

In addition, we have found that the selected active sites on the basal surface model of graphite exhibit active catalytic reactivity toward the dissociation of CO and C₂H₂ and the chemical adsorption can occur at close intervals to the basal graphite surface.

Acknowledgments. The authors gratefully acknowledge partial financial support from the research council of Alzahra University and Shahid Rajaee Teacher Training University.

REFERENCES

1. Li Q., Yan H., Zhang J. *et al.* // Carbon. – 2004. – **130**. – P. 829 – 835.
2. Westberg H., Boman M., Norekrans A.S. *et al.* // Thin Solid Films. – 1992. – **215**. – P. 126 – 133.
3. Antes J., Hu Z., Zhang W. *et al.* // Carbon. – 1999. – **37**. – P. 2031 – 2039.
4. Li W.Z., Xie S.S., Qian L.X. *et al.* // Science. – 1996. – **274**. – P. 1701 – 1703.
5. Kuc A., Heine T., Seifert G. // Phys. Rev. – 2010. – **B81**. – P. 085430 – 085437.
6. Podeszwa R. // J. Chem. Phys. – 2010. – **132**. – P. 044704 – 044802.
7. Hock K.M., Barnard J.C., Palmer R.E. *et al.* // Phys. Rev. Lett. – 1993. – **71**. – P. 641 – 644.
8. Janiak C., Hoffmann R., Sjovald P. *et al.* // Langmuir. – 1993. – **9**. – P. 3427 – 3440.
9. Jensen F. Introduction to Computational Chemistry, Wiley VCH, Chichester, UK, 1999.
10. Chen N., Yang R.T. // Carbon. – 1998. – **36**. – P. 1061 – 1070.
11. Chen N., Yang R.T. // J. Phys. Chem. A. – 1998. – **102**. – P. 6348 – 6356.
12. Bennett A.L., McCarroll B., Messmer R.P. // Phys. Rev. B. – 1971. – **3**. – P. 1397 – 1406.
13. Dewar M.J.S., Zoebisch E.G., Healy E.F. *et al.* // J. Amer. Chem. Soc. – 1985. – **107**. – P. 3902 – 3909.
14. Stewart J.J.P. // J. Comput. Chem. – 1989. – **10**. – P. 221 – 264.
15. Stewart J.J.P. // J. Comput. Chem. – 1989. – **10**. – P. 209 – 220.
16. Stewart J.J.P. // J. Mol. Model. – 2007. – **13**. – P. 1173 – 1213.
17. Gordon M.H., Pople J.A. // Chem. Phys. Lett. – 1988. – **153**. – P. 503 – 506.
18. Hehre W.J., Ditchfield R., Pople J.A. // J. Chem. Phys. – 1972. – **56**. – P. 2257 – 2261.
19. Clark T., Chandrasekhar J., Schleyer P.v.R. // J. Comp. Chem. – 1983. – **4**. – P. 294 – 301.
20. Krishnam R., Binkley J.S., Seeger R. *et al.* // J. Chem. Phys. – 1980. – **72**. – P. 650 – 654.
21. Gill P.M.W., Johnson B.G., Pople J.A. *et al.* // Chem. Phys. Lett. – 1992. – **197**. – P. 499 – 505.
22. Voityuk A.A., Rosch N. // J. Phys. Chem. A. – 2000. – **104**. – P. 4089 – 4094.
23. Thiel W., Voityuk A.A. // Theor. Chim. Acta. – 1992. – **81**. – P. 391 – 404.
24. Thiel W., Voityuk A.A. // J. Phys. Chem. – 1996. – **100**. – P. 616 – 626.
25. Boys S.F., Bernardi F. // Mol. Phys. – 1970. – **19**. – P. 553 – 566.
26. Schmidt M.W., Baldridge K.K., Boatz J.A. *et al.* // J. Comput. Chem. – 1993. – **14**. – P. 1347 – 1363.
27. MOPAC2009, James J.P. Stewart, Stewart Computational Chemistry, Version 8.331M, Colorado springs, USA, 2009.
28. Xu S.C., Irle S., Musaev D.G. *et al.* // J. Phys. Chem. A. – 2005. – **109**. – P. 9563 – 9572.
29. Xu S.C., Irle S., Musaev D.G. *et al.* // J. Phys. Chem. B. – 2006. – **110**. – P. 21135 – 21144.
30. Matsubara T., Maseras F., Koga N. *et al.* // J. Phys. Chem. – 1996. – **100**. – P. 2573 – 2580.
31. Porezag D., Frauenheim T., Koehler T. *et al.* // Phys. Rev. B. – 1995. – **51**. – P. 12947 – 12957.
32. Elstner M., Hobza P., Frauenheim T. *et al.* // J. Chem. Phys. – 2001. – **114**. – P. 5149 – 5155.
33. Nic M., Jirat J., Kosata B. Rice—Ramsperger—Kassel—Marcus (RRKM) theory, Blackwell Scientific Publications, Oxford, UK, 1997.
34. Zhang Y.H., Chen Y.B., Zhou K.G. *et al.* // Nanotechnology. – 2009. – **20**. – P. 185504 – 185512.
35. Lee C., Yang W., Parr R.G. // Phys. Rev. B. – 1988. – **37**. – P. 785 – 789.